Journal of Micromechatronics, Vol. 3, No. 3–4, pp. 239–266 (2006)

Also available online - www.vsppub.com

Networked human/robot cooperative environment for tele-assembly of MEMS devices

YANTAO SHEN [1,*], NING XI [1], BOOHEON SONG [1], WEN J. LI [2] and CRAIG A. POMEROY [1]

[1] *Department of Electrical and Computer Engineering, Michigan State University, East Lansing, MI 48824, USA*
[2] *Department of Automation and Computer Aided Engineering, The Chinese University of Hong Kong, Shatin, Hong Kong, China*

Abstract—The objective of this paper is to develop a networked cooperative environment to achieve human/robot cooperation for reliable and dependable remote microassembly. At a microscale, surface adhesion forces, such as van der Waals, surface tension and electrostatic forces, become stronger than the downward gravitational force. For a reliable and dependable tele-microassembly, it is absolutely necessary to allow close monitoring of the magnitude and direction of those micro-forces interacting with microdevices during the assembly process. In this paper, based on integrating an *in situ* polyvinylidene fluoride piezoelectric micro-force sensing tool with a resolution in the range of μN, and using event-synchronization for the feedback of assembly video and micro-force, the developed networked human/robot cooperative platform can greatly advance applications in tele-microassembly. As a result, the reliable and dependable human/robot cooperative assembly operations can be achieved and extended to the single or multiple remote work-cells through a local area network or the Internet. This platform has been used successfully to perform a remote assembly of surface MEMS structures with the event-synchronized micro-force/visual feedback *via* the Internet between USA and Hong Kong.

Keywords: Human/robot cooperation; network; Internet; teleoperation; synchronization; polyvinylidene fluoride; MEMS; micro-force sensor; microassembly; micromanipulation; micromanufacturing.

1. INTRODUCTION

Recent developments on micro/nano technologies and manipulations are extending the natural human environment to a whole new world at microscale, which allows potential impacts on micro handling/manipulation/assembly of small industrial

*To whom correspondence should be addressed. Tel.: (1-517) 432-1375. Fax: (1-517) 353-1980. E-mail: shenya@egr.msu.edu

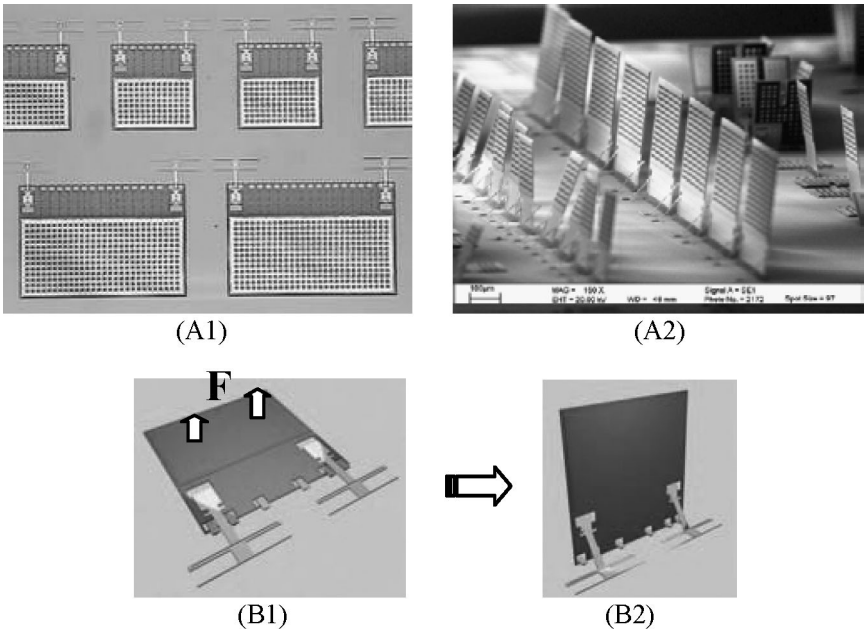

Figure 1. (A1) Microscope image of micro-mirror array on the chip, (A2) SEM picture of assembled micro-mirror array, (B1) the force is applied at the mirror, (B2) the automatic latches lock the mirror in upright position.

devices [1–14]. Unfortunately, processes capable of reliably assembling micro-devices have not been developed yet, partially because at the micro-scale structures are small, fragile and easily breakable [1]. Typically, the micro-mirror components are surface optomechanical structures. They lie on the surface of the substrate after the fabrication process, as shown in Fig. 1A1. An assembly process illustrated in Fig. 1B1 and 1B2 is needed to lift them up to a perpendicular position to serve as the optical switches, as shown in Fig. 1A2. However, due to the lack of micro-force feedback, the misadjusted assembly forces are often over the safe margin of micro-mirrors and easily break them during the operation. As a result, this situation decreases overall yield and drives up cost significantly [15].

Currently, the state-of-the art in complex microassembly is still a rather manual serial approach [16, 17]. Microdevices requiring complex manipulation are assembled by hand using an optical microscope and probes or small tweezers. However, like the assembly of micro-mirrors mentioned above, those operations are inherently risky without knowledge of the micro-force(s) being applied and due to the lack of effective interaction or reliable cooperation between human and robots. Therefore, to improve the reliability and dependability of microassembly and, more importantly, high sensitivity and high resolution, a micro-force sensing modality must be used [14]. It can be seen that, among the existing micro-force sensing techniques [2], very few of them can meet the requirements for assembly of such microdevices as the micro-mirrors in the μN level. In summary, for strain gauges [18], piezore-

sistive effect sensors [5], piezomagnetic effect sensors [19] and capacitive sensors, microdevices may generally offer sensing resolutions in the range of sub-mN or mN. Although optical techniques have high resolution in the nN range [8], compared to other methods they are more expensive and have less dynamic range. Fortunately, the piezoelectric material polyvinylidene fluoride (PVDF) has been explored to have many advantages and potentials when used to design a high sensitivity force sensor at the μN level. In this paper, we design such a micro-force sensing tool based on the piezoelectric effect for microassembly. Moreover, by integrating this PVDF micro-force sensing tool into a micromanipulator, the micro interaction forces between the microdevices and the micromanipulator can be accurately achieved; then, the cooperation between human operator and micro-robots can be enhanced so as to achieve a reliable and dependable microassembly.

In addition, some recent efforts on implementation of micromanipulation *via* a local are network (LAN) or the Internet may allow potential impacts and efficiency on the micro-assembly/manufacturing industrial area [7]. However, this tele-micro manipulation/assembly becomes significantly challenging due to the certain performance characteristics. That is, the random time delay, latency, jitter, network buffering effects and disconnections experienced over the network or Internet present major difficulties. Those difficulties, especially resolving time delay effects in the teleoperation systems with force/haptic feedback in the macro environment, have been extensively studied in many works, for example, using the scattering theory formalism in Ref. [20] and the shared compliant control in Ref. [21]. However, all these studies have had several limitations, since they assume the time delay to be either fixed, the same in both directions, or having an upper bound, none of which applies to a long-distance network or Internet time delay. Moreover, microassembly/handling/manipulation is a high-precision task. The synchronization of all feedback streams such as force/position, video and others becomes much more necessary for feasibility and safety of micro operations. Therefore, there is a need for a telemicroassembly methodology that can achieve stability, synchronization and transparency of networked or Internet-based teleoperation, regardless of the time delay and its variance. Recently, several efforts have been reported in the force reflecting micromanipulation. They applied the H_∞ optimal control theory and μ-synthesis method to achieve a robust bilateral operation when the time-delay margin was pre-specified and the force scaling was considered [7, 10]. Besides these developed time-based methodologies, event-based planning and control was first introduced by one of the authors of this paper in Ref. [22] and implemented with an Internet based telerobot in real-time with force feedback in Refs [23, 24]. The basic concept of an event-based approach is to use event as a reference for the different system entities rather than the traditional time-based Internet operations [22]. This method does not avoid or eliminate random and unbounded delay. Instead, the event-based method allows for unexpected or uncertain delays and uses that delay to adjust or modify the original control plan to form the desired input. Since the event-based method is not a function of time, the system is immune to time delay and elim-

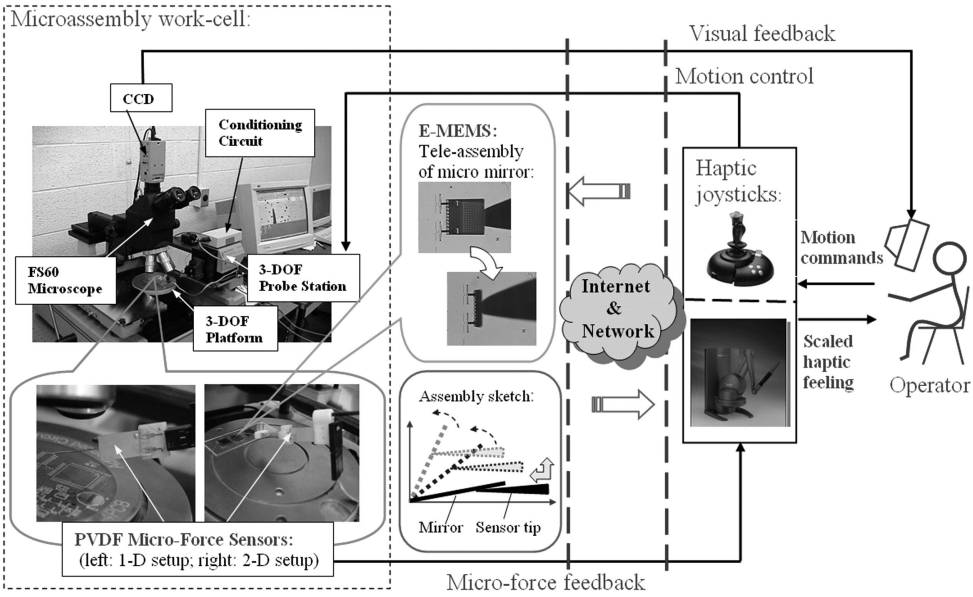

Figure 2. Networked human/robot cooperative environment for tele-microassembly.

inates the buffering effect of delay. It has been proven local area network CLAN that event-based method can provide stable, robust performance [24]. As a result, this method has been employed and improved in our paper so as to achieve an effective event-synchronization of the video and micro-force for the developed system.

In this paper, based on the developed high-sensitivity PVDF micro-force sensing tool and the event-synchronization approach as shown in Fig. 2, we developed a networked human/robot cooperative environment which attempts to reach the utmost integration of heterogeneity of human and robot functions for achieving reliable and dependable teleassembly of microdevices.

In this tele-microassembly environment, more importantly, human perception is matched with robot sensory measurements such as the μN range micro-force and magnified vision, and then a remote sensing and interactive platform for the human/robot cooperative operations in micro-scale environments is provided or enhanced. Since the dominant physical quantities in the micro world are different from those of the macro-world, the capture and feedback of micro-interaction forces are the keys to achieve the reliability and dependability of human/robot cooperative microassembly. Moreover, since video can be event-synchronized with the micro-force, the reliable and dependable human/robot cooperative assembly operations can be robustly achieved and extended to the single or multiple remote work-cells through LAN or the Internet.

This human/robot cooperative platform has been successfully used to perform a tele-assembly of surface MEMS–micro-mirrors with the event-synchronized micro-force and visual feedback *via* the Internet between the USA and Hong Kong. The implementations and experimental results have clearly demonstrated the advantages

of the developed human/robot cooperative platform, such as greatly improved reliability and dependability of microassembly. This platform could be an important step towards enabling reliable and high yield batch fabrication and remote assembly of MEMS.

This paper is organized as follows. Section 2 reviews the design and modeling, the signal processing unit and calibration of the PVDF piezoelectric force sensing tool. Event-based human/robot tele-microassembly platform is detailed in Section 3. Section 4 demonstrates the tele-microassembly experimental results, especially force-reflecting microassembly of micro-mirrors with event-synchronization *via* the Internet between USA and Hong Kong. Finally, we conclude the work in Section 5.

2. FORCE SENSING FOR HUMAN/ROBOT COOPERATIVE MICROASSEMBLY

In the human/robot cooperative microassembly environment, human actions are usually based on human perception. To improve the human/robot cooperation for reliable microassembly, a perceptive microassembly to match human perception with the robot sensory information such as micro-force is the key for combining human reasoning/command with micro robot autonomous planning/control.

2.1. Micro-force sensing tool design

To achieve micro-force sensing for human/robot cooperative microassembly, we use PVDF in the design of the high-sensitivity force sensor. PVDF, as a piezoelectric material, has a relatively low modulus of elasticity, relatively high electromechanical coupling coefficient and relatively low cost [25]. These properties make the PVDF piezoelectric polymer an ideal force transduction material for micro-force sensing. Besides our work, several micro-robotic applications using piezoelectric PVDF have been briefly presented without theoretical analysis of the force sensing mechanism [26].

The structure shown in Fig. 3 illustrates a 1D PVDF micro-force sensor. The sensor is designed with a composite beam whose piezoelectric layer acts as a sensing

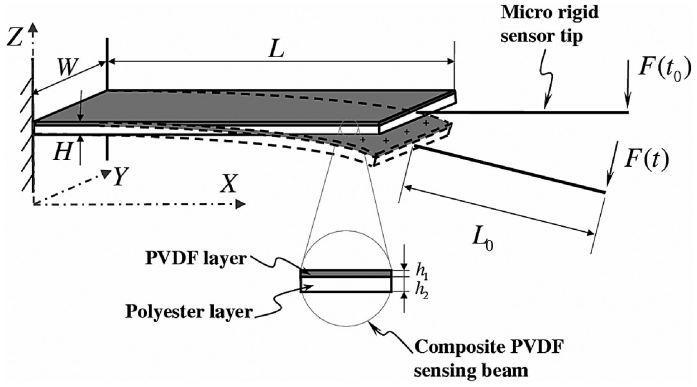

Figure 3. Illustration of the 1D sensor structure.

device bonded to a polyester support beam layer. The deformation of the sensing beam is caused by the applied force acting at the free end of the rigid tip. Since the sensor is exactly a micro tool with force sensing, and can be used to manipulate the microdevice, the sensor is also called the micro-force sensing tool in this paper.

Based on the piezoelectric effect [27], the mechanics of the materials for the cantilever beam [28], and an equivalent circuit model of a resistor R_P in parallel with a capacitor C_P for the PVDF film, the output voltage $V(t)$ across the PVDF film due to charge $Q(t)$ generated by the external micro-force $F_c(t)$ can be described by [29]:

$$\frac{V(t)}{R_P} + \dot{V}(t)C_P = \frac{dQ}{dt}. \tag{1}$$

Thus, we have the following equation to represent the relationship between the generated voltage and the contact force:

$$V(t) + \lambda \dot{V}(t) = B\dot{F}_c(t), \tag{2}$$

where $\lambda = R_P C_P$ is a time constant and

$$B = \frac{R_P d_{31} A\left(L_0 + \frac{L}{2}\right)c}{I}$$

is a constant. A is surface area ($L \times W$), d_{31} is transverse piezoelectric coefficient, I denotes the inertial moment of cross-sectional area $A_c(W \times (h_1 + h_2))$ of the composite PVDF sensing beam and c is the distance between the PVDF layer and the neutral axis of the sensing beam.

By Laplace transformation, the electrical transfer function of the sensor is given as:

$$T(s) = \frac{V(s)}{F_c(s)} = \frac{B}{\lambda}\frac{\lambda s}{1 + \lambda s}. \tag{3}$$

This formulation implies the open-circuit sensor model is indeed a high-pass filter.

To follow the 1D sensor model, a self-decoupling 2D PVDF force sensor has been designed, as shown in Fig. 4.

In addition, the 2D sensor is designed based on a parallel beam structure. In each direction, a 2-piece parallel beam with a gap d is used to improve the rigidity of the structure and, at the same time, maintain the sensitivity of the force sensing in that direction (the sensing area is doubled due to the use of two PVDF films). It can also be seen that this structure provides decoupled force measurements in both the x(push-forward) and z (lift-up) directions. The decoupled output voltages and forces can be described as

$$\begin{aligned} V_z(t) + \lambda_z \dot{V}_z(t) &= B_z \dot{F}_z(t), \\ V_x(t) + \lambda_x \dot{V}_x(t) &= B_x \dot{F}_x(t), \end{aligned} \tag{4}$$

where $\lambda_z = \lambda_x = R_P C_P$. Similar to the 1D parameter, B_z and B_x are the constants.

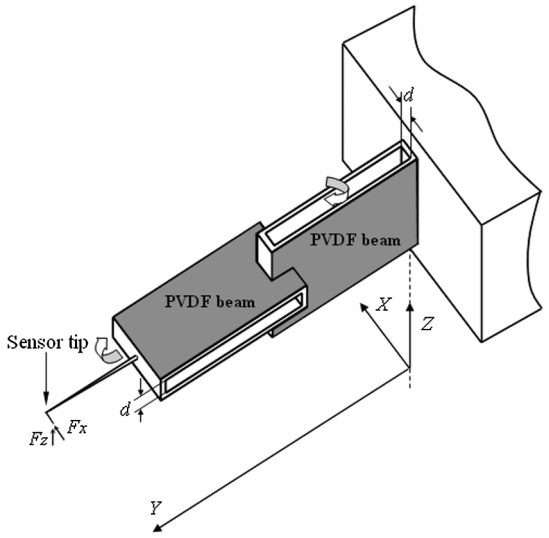

Figure 4. Illustration of the 2D force sensor structure.

2.2. Signal conditioning and interface circuit

For the micro-force signal conditioning, a differential charge amplifier with identical feedback capacitors C_{f1} and $C_{f2}(C_{f1} = C_{f2})$ was designed for the PVDF force sensor. The differential charge amplifier is based on the TC7650C chopper stabilized operational amplifier with high input impedance (10^{12} Ω) and low bias current (1.5 pA). Following the charge amplifier, a differential-to-single-ended amplifier with the gain K_c is added. Furthermore, by choosing the charge amplifier, the cable capacitances C_c are removed from the dynamic model of the circuit and a long cable can be used to connect the sensor and the circuit without affecting the system sensitivity. The small cable resistors R_{c1} and R_{c2} can further provide electrostatic discharge (ESD) protection. In this design, the total differential topology can efficiently reduce the common mode noise. To reject the existing high-frequency noise, an active low pass filter with a small time constant τ_1 is used before the voltage output. The integration of the output voltage by time can also be achieved by an integrator unit in the circuit. To further remove the noise from the data acquisition system, a Gaussian low pass filter and a 60 Hz notch filter are added in the data collection program. Moreover, the whole circuit is shielded. The operational amplifier casing is well grounded and the inputs are guarded and connected to the same ground as the casing. The simplified diagram of the developed circuit is shown in Fig. 5.

2.3. System transfer function

Finally, by considering the whole system (the sensor and the circuit), the global transfer function of the 1D sensor is

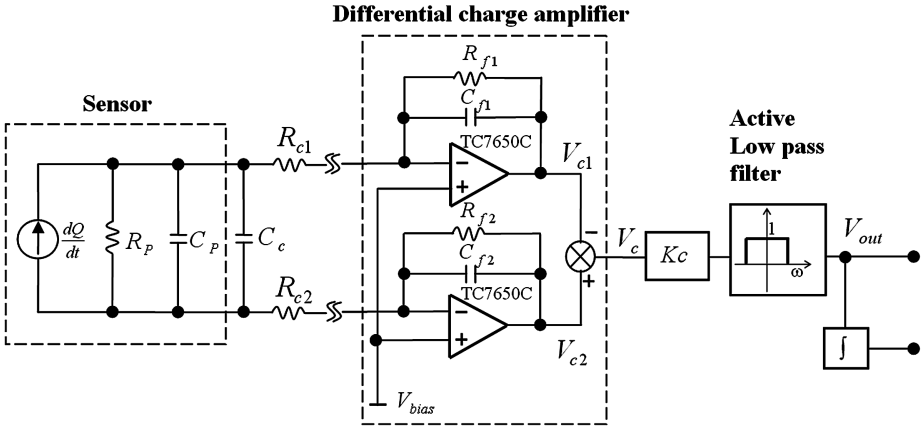

Figure 5. Schematics of the developed electronic interface circuit.

$$\begin{aligned} \mathrm{GT}(s) &= V_{c2}(s) - V_{c1}(s) \\ &= \frac{V_{out}(s)}{V(s)} \underbrace{\frac{V(s)}{F_c(s)}}_{T(s)} \\ &\doteq \frac{2K_cB}{R_PC_f} \frac{\tau s}{(1+\tau s)(1+\tau_1 s)}. \end{aligned} \tag{5}$$

The function is a bandpass filter, where $\tau = R_fC_f$ ($R_{f1} = R_{f2} = R_f$, $C_{f1} = C_{f2} = C_f$) is the time constant of the feedback loop in the charge amplifier. For force actions with an angular frequency range between $1/\tau$ and $1/\tau_1$, the output voltage of this bandpass filter would be roughly linearly proportional to the force. However, for force actions with angular frequency content below $1/\tau$, the output voltage would be proportional to the rate of the micro-force. Thus, for the latter force frequency range, an integration function circuit will be suitable. Here, since τ_1 is very small in the circuit (i.e., 0.001), equation (5) can be rewritten as

$$\mathrm{GT}(s) = \frac{V_{out}(s)}{F_c(s)} \doteq \frac{2K_cB}{R_PC_f} \frac{\tau s}{1+\tau s}. \tag{6}$$

From this equation, we can obtain the micro-force or force rate by measuring the output voltage of the 1D sensor system when the initial values $F_c(t_0)$and $V_{out}(t_0)$ are known, that is,

$$F_c(t) - F_c(t_0) = \frac{C_f}{2K_cBC_P}\left[\tau(V_{out}(t) - V_{out}(t_0)) + \int_{t_0}^{t} V_{out}(t)\mathrm{d}t\right]. \tag{7}$$

2.4. Vision-based calibration

By virtue of a precisely calibrated Mitutoyo 100× microscope (with a 50× objective and a 2× zoom) and a Sony CCD camera system, the vision-based calibration set-up for accurately measuring the tiny bending angle or deflection of the sensor beam under the microscope was built [29, 30]. After the vision measurements, the strain energy method of the bending cantilever beam [28] was employed to solve the calibration force. The calibration is based on the PVDF sensor beam (1D) has the following dimensions and parameters: $L_0 = 0.0225$ m, $L = 0.0192$ m, $W = 0.0102$ m, $h_1 = 28\ \mu$m, $h_2 = 125\ \mu$m, $R_P = 1.93 \times 10^{12}\ \Omega$, $C_P = 0.90 \times 10^{-9}$ F, $d_{31} = 23 \times 10^{-12}$ C/N. The Young's moduli of PVDF and polyester are 3×10^9 N/m^2 and 3.89×10^9 N/m^2, respectively, $R_f = 12 \times 10^9\ \Omega$ and $C_f = 390 \times 10^{-12}$ F. The setting of K_c may vary with different tasks. The diameter of the rigid tip of the sensing tool is about 55 μm. To reduce vibrations, an active vibration isolated table was used during the calibrations and experiments. Notice that, in this paper, all calibrations and experiments were implemented at stable room temperature. Figure 6 shows the comparison curves between the calibration forces and the theoretical forces using equation (7). The curves are close, which clearly indicates the effectiveness of the developed sensing models. By preliminary calibration, when $K_c = 480$, the sensitivity of the 1D PVDF sensory system was estimated to be 4.6602 V/μN, the 2D sensory system was 2.3985 V/μN (when the gap d is zero). The resolution of the sensor was in the range of μN. The output dynamic range of the sensor is 84.3 dB. When deflection of the sensor tip approaches 90°, the input dynamic range of the 1D sensor was estimated to be more than 82.29 dB, while the 2D sensor was about 121.9 dB. The working frequency of the used sensor in this paper is from 0.034 to 160 Hz. The accuracy of the 1D sensor in the full-scale (angle 0–0.035) was estimated to be ±11.92%.

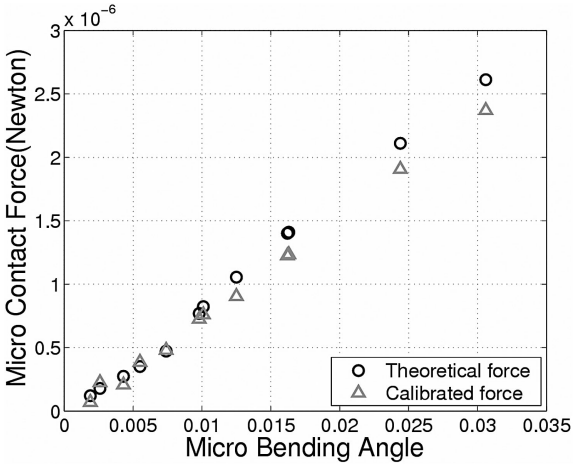

Figure 6. Comparison of theoretical and calibrated forces.

2.5. Sensing tests

To demonstrate sensor performance, a contact-stop sensing experiment was implemented, where the 2D sensor tip was controlled to contact on a planar glass surface. The surface was set up at an angle of 75° around y with respect to the z–y plane, as shown in Fig. 7. This set-up means $F_z = F\cos 15°$ and $F_x = F\cos 75°$. The 2D force signals recorded are plotted in Fig. 8 ($F_z \approx 3.7F_x$ in the plot). The result verifies the performance of sensing and self-decoupling of the 2D force sensor.

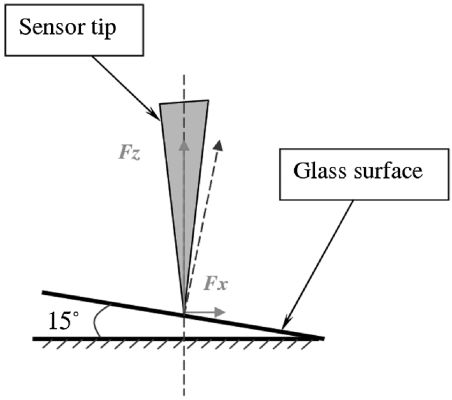

Figure 7. The test set-up of the 2D force sensing.

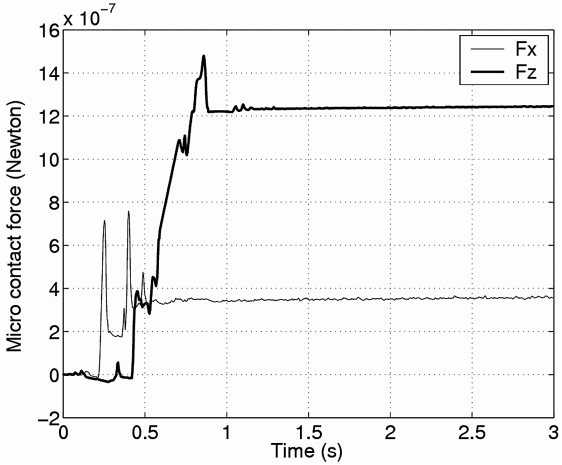

Figure 8. 2D sensor responses with a force applied at a 75° angle with respect to the z–y plane.

3. EVENT-BASED HUMAN/ROBOT TELE-MICROASSEMBLY SYSTEM

3.1. System integration and architecture

Microssembly requires operations to be performed under a microscope. The visual information on the position of the robot and the surrounding workspace can be updated through video feedback to the human operator. By visually observing the assembly operations, a human can plan and correct the next operation so as to achieve a reliable and robust assembly. In this paper, we used both the micro-force and vision as essential action references for an integrated human/robot cooperative system. That is, the developed piezoelectric PVDF force sensing tools with a resolution in the range of μN can be integrated with a micromanipulator. The Mitutoyo FS60 optical microscope and a Sony SSC-DC50A CCD Color Video Camera can capture the microassembly process in realtime, and feed back the visual information. The integrated microassembly work-cell in the Robotics and Automation Laboratory at Michigan State University is shown in Fig. 9. It consists of a 3-DOF micromanipulator (SIGNATONE Computer Aided Probe Station), a 3-DOF platform, a Mitutoyo FS60 optical microscope and a Sony SSC-DC50A CCD Color Video Camera. The 3D platform can be controlled to convey the microdevices to the working area observed by the microscope. To reduce vibrations, an active vibration isolated table is used during microassembly. The joystick used in the human/robot cooperative microassembly system can be a 3-DOF Microsoft SideWinder force feedback joystick or a 6-DOF Phantom joystick.

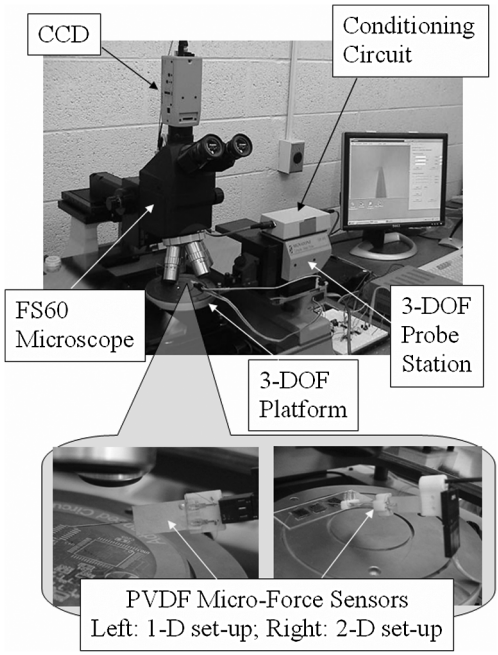

Figure 9. Human/robot integrated microassembly work-cell at MSU.

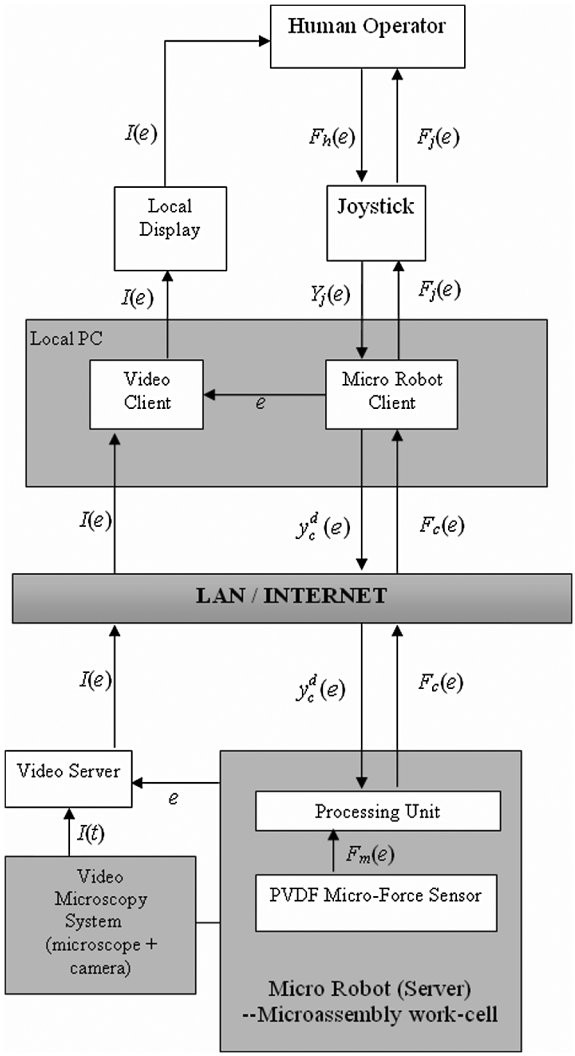

Figure 10. Event-based system architecture.

Consequently, the developed event-based architecture of this tele-microassembly system is shown in Fig. 10. In the architecture, e denotes the event reference, t represents the time reference. To realize the synchronization of all feedback streams, a video server tags each video frame with the event reference e and forwards it to the video client. Before displaying a frame, the video client compares its event reference with the event reference of the force and position currently being rendered in the robot client. If the video frame's event reference is much less than the force's event reference, then the frame is discarded. This is related to the event-synchronization approach and will be detailed in Section 3.4. In the architecture, VIC [31] was used as both video server and client. VIC was developed

by the Network Research Group at the Lawrence Berkeley National Laboratory in collaboration with the University of California, Berkeley. VIC is flexible and readily adapted to this system. It can handle a variety of codes, such as MPEG and JPEG, and many different kinds of image capturing devices. In our system, VIC was modified to obtain event references from a robot server and a robot client and to tag an event reference to each video frame. The robot and video clients are placed in the same local PC. The robot client places an event reference into shared memory to be collected by the video client.

3.2. Human/robot dynamic characteristics and control scheme

To implement the developed system, it should be emphasized that the human dynamic characteristics play an important role in the performance of the human/robot system. A human action is planned and controlled at the task level. The basic human motions are linear, following a spring-like behavior [32]. In addition, a human can compensate for certain machine instabilities making the coupled human/robot system stable [33]. From the architecture shown in Fig. 10, when the human operator operates the joystick, the dynamic model of the human/joystick is simplified as a spring-mass-damping system:

$$M_{\mathrm{m}}\ddot{Y}_{\mathrm{j}}(e+1) + B_{\mathrm{m}}\dot{Y}_{\mathrm{j}}(e+1) + K_{\mathrm{m}}Y_{\mathrm{j}}(e+1) = F_{\mathrm{h}}(e) + F_{\mathrm{j}}(e), \tag{8}$$

where M_{m} is the mass of the joystick handle, B_{m} is the damping coefficient of the joystick, K_{m} is the spring constant, e is the event, $F_{\mathrm{h}}(e)$ is the force applied by the operator, $F_{\mathrm{j}}(e)$ is the scaled reflective force from the micro-force sensor of the micromanipulator and $Y_{\mathrm{j}}(e+1)$, $\dot{Y}_{\mathrm{j}}(e+1)$ and $\ddot{Y}_{\mathrm{j}}(e+1)$ are the joystick position, velocity and acceleration, respectively. The joystick position $Y_{\mathrm{j}}(e+1)$ at the event $e+1$ is generated by the previous force at event e. This results in an event-based system where each event is triggered by the previous one. In order to obtain a unified human/robot action model and control structure, it is also essential to compensate for the nonlinearity of micro robot (micromanipulator) dynamics and to be able to control the microrobot action at a task level. The joint space dynamic and kinematic equations for a generic micro robot/manipulator with n degrees of freedom are given by

$$\begin{cases} H(q)\ddot{q} + C(q,\dot{q}) + G(q) = \tau_{\mathrm{r}} - J^{\mathrm{T}}(q)F_{\mathrm{c}}, \\ y = h(q), \end{cases} \tag{9}$$

where F_{c} is the output force from the sensor in the task space, and $h(q)$ represents the forward kinematics, τ_{r} is the torque applied by the actuators, q is the joint angle of the micro robot and J is the Jacobian matrix of the microrobot. Notice that, in our system, the micromanipulator is a 3-DOF probe driven by 3 precision linear motors with a step resolution of 32 nm. The detailed dynamic and kinematic equations of the manipulator (including the sensor dynamic models) can be found in our previous work [29, 34, 35]. In this paper, the presented dynamic model and control method here are subject to the applications of generic robotic manipulator.

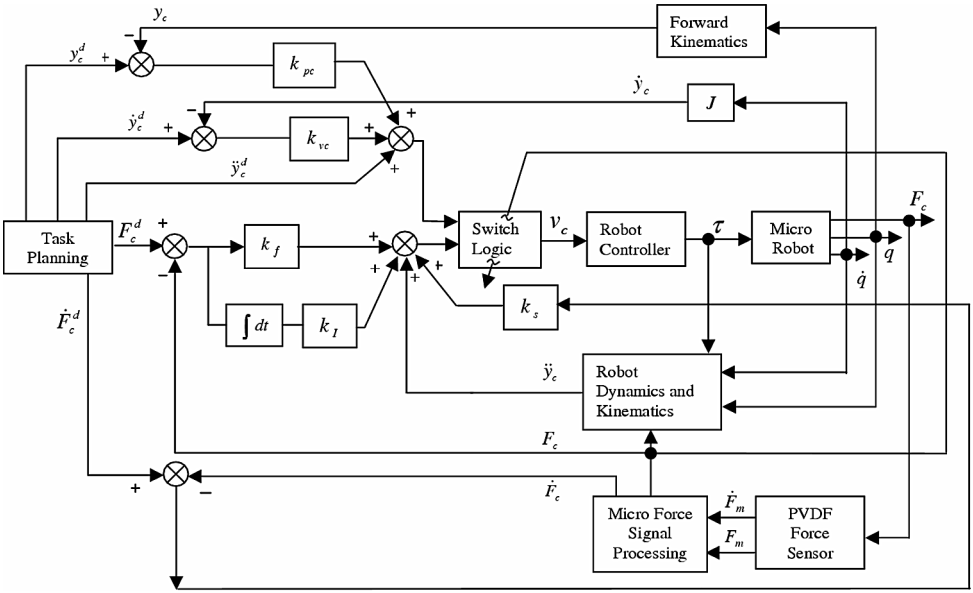

Figure 11. Control scheme for sensor-based micro robot.

Equation (9) introduces the non-linear feedback control law:

$$\tau_{\mathrm{r}} = H(q)J^{\#}(q)\big(\upsilon - \dot{J}(q)\dot{q}\big) + C(q,\dot{q}) + G(q) + J^{\mathrm{T}}(q)F_{\mathrm{c}}, \tag{10}$$

where $J^{\#}(q)$ is the pseudo-inverse of the Jacobian matrix. As a result, the dynamics of the micromanipulator can be linearized and decoupled as

$$\begin{aligned} \ddot{y}_{\mathrm{u}} &= \upsilon_{\mathrm{u}}, \\ \ddot{y}_{\mathrm{c}} &= \upsilon_{\mathrm{c}}, \end{aligned} \tag{11}$$

where y_{u} represents the output positions and orientation in the unconstrained directions and y_{c} represents the output positions and orientation in the constrained directions. Obviously, the control in the unconstrained directions will not have an effect on dynamics in the constrained directions and vice versa.

Following the linearized microrobot dynamics, the planning and control scheme of the microrobot was developed and is illustrated in Fig. 11. Referring to the event-based architecture, for the position control of the sensor tip in the constrained directions, we have

$$\upsilon_{\mathrm{c}}(e) = \ddot{y}_{\mathrm{c}}^{d}(e) + k_{\upsilon\mathrm{c}}\big(\dot{y}_{\mathrm{c}}^{d}(e) - \dot{y}_{\mathrm{c}}(e)\big) + k_{\mathrm{pc}}\big(y_{\mathrm{c}}^{d}(e) - y_{\mathrm{c}}(e)\big), \tag{12}$$

where $k_{\upsilon\mathrm{c}}$ and k_{pc} are the gains, and y_c^d is the scaled position command from human to the microrobot.

Notice that in this control scheme, the measurement of acceleration is required. However it will be difficult to obtain a real-time acceleration measurement. Therefore, we propose to use the prior value of the acceleration calculated from equa-

tion (9) to replace the real-time value. This method has been used in several applications with satisfactory results [29, 35].

3.3. Scaling law

To improve the dexterity and maneuverability of the human operator, scaling between micro and human environments' force and position has been carefully tuned and calibrated. Using the scaling factors, the relationships between the human and the microrobot in position and force are defined in a simplified form:

$$y_{\mathrm{c}}^{d}(e) = s_{\mathrm{p}} Y_{\mathrm{j}}(e), \tag{13}$$

and

$$F_{\mathrm{j}}(e) = s_{\mathrm{f}} F_{\mathrm{c}}(e), \tag{14}$$

where $Y_{\mathrm{j}}(e)$ is the position commands from the human to the joystick. $F_{\mathrm{j}}(e)$ and $F_{\mathrm{c}}(e)$ are the haptic force to human operator and the assembly force from the PVDF micro-force sensor, respectively. As the position scaling factor s_{p} is determined by the micro workspace geometry, it can be selected as a constant. To satisfy the human-joystick dynamics and to minimize the distortion of the micro workspace, the force scaling factor s_{f} can then be determined. Using the scaling laws mentioned above, both the microforce and movement are effectively scaled up and down between the joystick and micromanipulator.

3.4. Event-based synchronization

Since we consider micro-force and vision feedback in this cooperative teleassembly system, synchronization is another important feature for realizing reliable and dependable tele-microassembly. The current technology does not allow for perfect synchronization in networked teleoperation. The main limitations, which are communication related, are bandwidth and time delay. To improve synchronization of the developed networked human/robot cooperative environment to an acceptable level, the event-synchronization method was developed.

An event-synchronized system is one in which all the signals in the system are always referencing events which are within a certain tolerance range of each other. This implies that the system has to be designed in a way that the video and force/position being rendered have action reference stamps to guarantee the most current state of each other.

The event-synchronization approach presented here has all the features of inter-stream synchronization in the typical time based system, but uses event reference stamps instead of time stamps. This approach was realized based on the developed system architecture, as shown in Fig. 10. In the time-based synchronization, a traditional video server places a time stamp on each video frame and sends it to a video client. The client plays the video frames in the time stamp order. But in the event-based synchronization, a video server obtains an event reference e from the

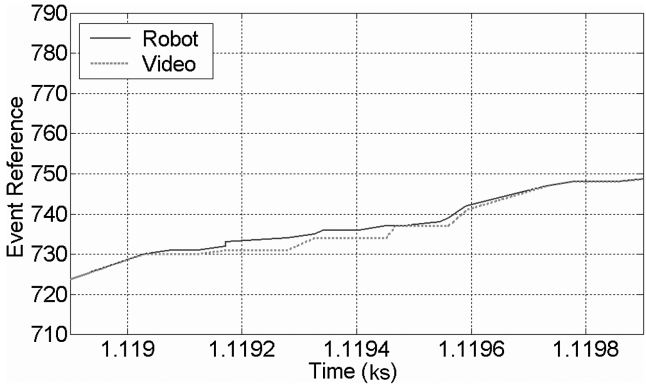

Figure 12. Event transfer behavior between force (robot client) and video (video client) *via* LAN without event-based synchronization.

micro-robot and attaches it to a video frame $I(t)$. Then the video server sends the event reference tagged video frame $I(e)$ to a video client. The video client obtains an event reference e of micro-force feedback $F_c(e)$ from the micro-robot client. Before the video client displays the video frame $I(e)$, the video client compares the event reference of the micro-force feedback $F_c(e)$ with the event reference of video frame $I(e)$. If the event reference of the video frame is substantially older than the event reference of the force feedback signal, the video client discards that frame. Usually, a video frame takes more time to transfer through a network than a force signal since a video frame contains much more information than the force feedback signal. Therefore, an event reference of the force feedback is never older than an event reference of the video frame at any time. In other words, since video feedback is always slower than micro-force feedback, depending on the network status and the size of the frame, a certain tolerance has to be allowed and set. That is, the video frame generated at event e can be rendered at any event reference within $e + N$, where N is acceptable tolerance. If the video frame does not arrive within this margin then it is discarded. Now what the operator will be seeing cannot be more N events older than what is being felt from force feedback. This results in the video feedback being event-synchronized with the micro-force/position feedback. Thus, the human operator can be sure that the feedback video display is close in event to the micro-force felt. This synchronized method enhances the reliability and dependability of the developed networked human/robot cooperative microassembly environment.

Several experiments have been done to compare the performance between the systems without/with event-synchronization. The first experiment is related to the comparison *via* LAN. The results show the synchronization effects between the force data in the robot client and the video frame in the video client. The variation between Fig. 12 and Fig. 13 shows different results, based on whether the event-based synchronization was used or not. Figure 12 shows that the event reference gap between the robot client and video client diverges in 4 events sometimes. As

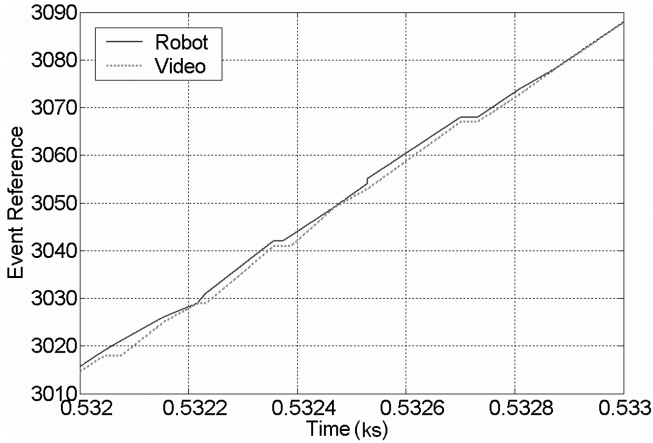

Figure 13. Event transfer behavior between force (robot client) and video (video client) *via* LAN with event-based synchronization.

stated previously, the divergence can be attributed to network delay. This implies that the latest video frame the operator received was not the video frame captured at the same moment the latest force feedback was generated by the micro robot. Because of this, the operator may lose the current operation status of the micro robot without using event-based synchronization. Using the event-synchronization, Fig. 13 shows the event reference gap between the robot client and video client to be smaller than 3 events. This is within the predefined tolerance (where $N = 3$). This implies that the latest video frame the operator saw was guaranteed to capture at the almost same moment the latest force feedback was generated by the robot. It can be seen that the two curves close each other in Fig. 13 and, additionally, they are quite linear. This means the video frame transfer is smooth like the force data transfer without being significantly affected by time delay. In this experiment, a TCP socket is used for communication connection. VIC setting is as follows: bandwidth = 128 kb/s, frames-per-second (fps) = 16, picture quality: 1. In addition, the networked system testing results for this experiment are as follows: (1) between robot server and video server: packet loss = 0%; approximate round trip times, minimum = 0 ms, maximum = 1 ms, average = 0.5 ms. (2) Between video client and video server: packet loss = 0%; approximate round trip times, minimum = 0 ms, maximum = 0 ms, average = 0 ms. (3) Between robot client and robot server: packet loss = 0%; approximate round trip times, minimum = 0 ms, maximum = 1 ms, average = 0.5 ms.

We also regularly compare the performance between the systems without/with event-synchronization *via* Internet. The Internet connection is between MSU, USA and Hong Kong, China. Figures 14 and 15 show quite different presentations. Figure 14 shows that the event reference gap between the robot client and the video client is not constrained. This gap between the robot client and the video client is caused by the Internet delay, which is random and unbounded. This implies

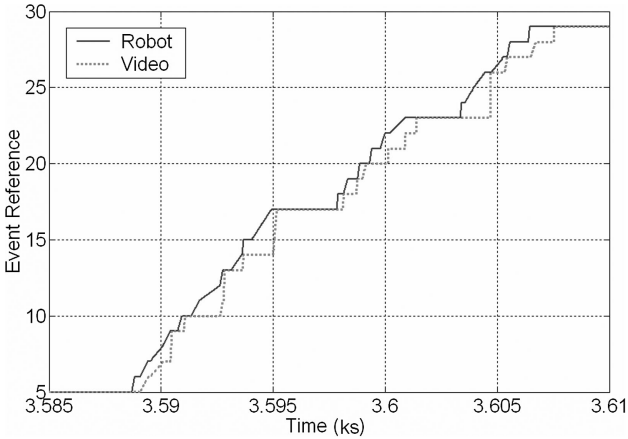

Figure 14. Event transfer behavior between force (robot client) and video (video client) *via* the Internet without event-based synchronization.

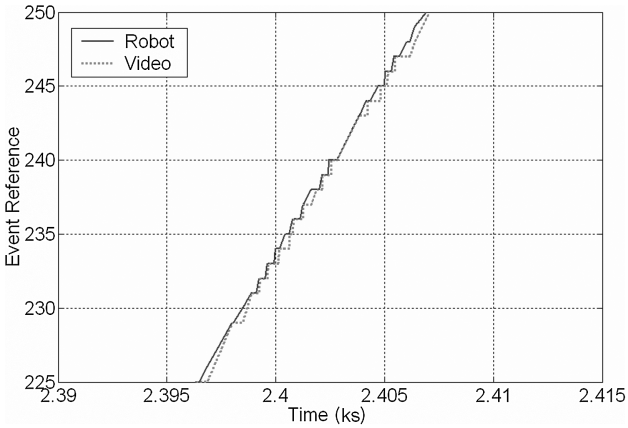

Figure 15. Event transfer behavior between force (robot client) and video (video client) *via* the Internet with event-based synchronization.

that the latest video frame the operator received was not the video frame captured at the moment of the latest force feedback the microrobot generated. Therefore, the operator can easily loose the current status of the microrobot. Looking at the performance of the event-synchronized system, as shown in Fig. 15, the largest event reference gap between the robot client and the video client was 1 event, which is the tolerance predefined for this experiment ($N = 1$). This implies that the latest video frame the operator saw was the video frame captured at the closest moment of the latest force feedback the robot made within the predefined tolerance. In Fig. 15, the transfer behaviors are also more linear and smooth than the system without event-synchronization. In this experiment, a TCP socket is used for connections. VIC setting is as follows: bandwidth = 3072 kb/s, fps = 30, picture quality = 1. The networked system testing results for this experiment are as follows: (1) between

robot server and video server: packet loss = 0%; approximate round trip times, minimum = 10 ms, maximum = 821 ms, average = 58 ms. (2) Between video client and video server: packet loss = 2%; approximate round trip times, minimum = 275 ms, maximum = 313 ms, average = 278 ms. (3) Between robot client and robot server: packet loss = 1%; approximate round trip times, minimum = 295 ms, maximum = 1046 ms, average = 346 ms.

In summary, with the event-based synchronization the operator has an assurance that all the feedback streams, such as force feedback and video, are rendered at the closest moment as if they are synchronized. In this way the effects of time delay are significantly reduced.

4. NETWORKED HUMAN/ROBOT COOPERATIVE MICROASSEMBLY OPERATIONS

As shown in Fig. 2 in Section 1, using the developed environment, we can reliably teleassemble MEMS devices such as micro-mirrors by hand *via* the LAN/Internet.

Several experiments on the teleassembly of the micro-mirrors have been done between USA and Hong Kong *via* the Internet. The detailed operation procedures on the teleassembly of a micro-mirror are as follows: before the lift-up, firstly, the operator drives the joystick to move the sensor tip to an initial position under the micro-mirror. Then the tip is operated to move forward and upward simultaneously. As a result, the moving tip begins to lift the micro-mirror up until the mirror approaches an upright position. With the assistance of the micro-force/haptic feedback, and the event-synchronized visual feedback from the microscope and camera, the task of remote microassembly *via* LAN/Internet can be achieved reliably and easily. Figure 16 gives an illustration of the assembly of a micro-mirror by the PVDF micro-force sensor tip.

Figure 17 shows the time *vs.* event behaviors of the robot server and the robot client during the teleassembly with event-synchronization (robot client was in the Chinese University of Hong Kong).

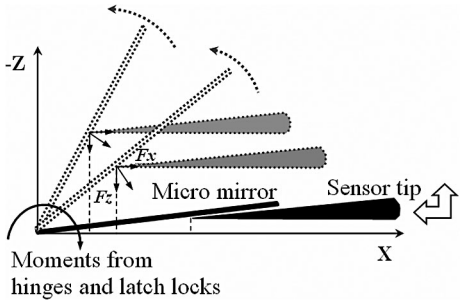

Figure 16. Assembly of micro-mirror by the sensor tip.

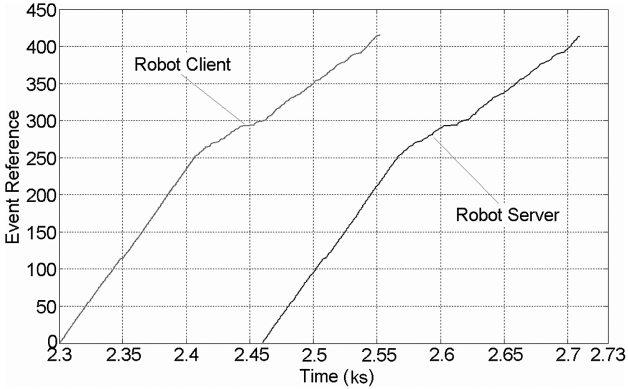

Figure 17. Time *vs*. event behavior of robot server (Michigan State University) and robot client (The Chinese University of Hong Kong).

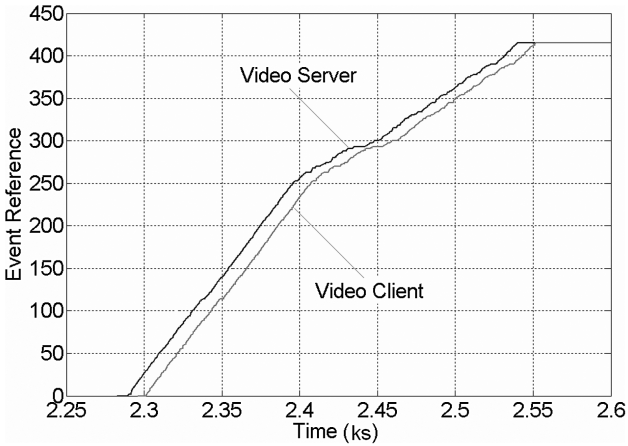

Figure 18. Time *vs*. event behavior of video server and client.

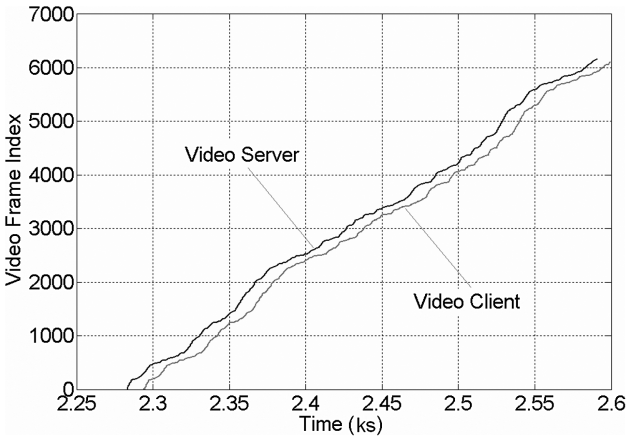

Figure 19. Time *vs*. video frame index behaviors of video sever and client.

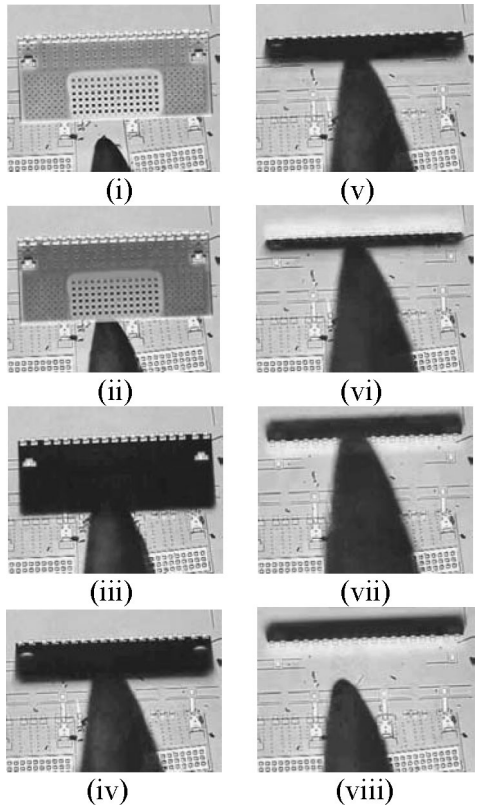

Figure 20. The feedback video sequence of networked tele-assembly of a micro-mirror between USA and Hong Kong using the Microsoft joystick and the 1D force sensor set-up.

Moreover, Figs 18 and 19 show the time *vs.* event behaviors and the time *vs.* video frame index behaviors of the video server and client during the event-synchronized tele-assembly, respectively.

From the event behavior results shown above, the event behavior of robot client in Fig. 17 and the event behavior of video client in Fig. 18 are close. This means event-synchronization is in action for the teleassembly of micro-mirrors *via* Internet. Here, VIC setting for the following experiments is: bandwidth = 3072 kb/s, fps = 30, picture quality = 3, predefined tolerance is $N = 2$.

Figure 20 shows one of the reliable and successful assembly sequences of the micro-mirror using the developed networked human/robot cooperative environment between USA (workcell side) and Hong Kong (operator side, using Microsoft joystick) *via* the Internet. The 1D PVDF micro-force sensor set-up was employed. The gain K_c of the sensor amplifier was set as 48. The size of the micro-mirror used is about 600 μm $\times$ 250 μm. In this assembly, the microscope was set with a 20$\times$ objective lens. The force scale factor s_f was 3.8×10^5.

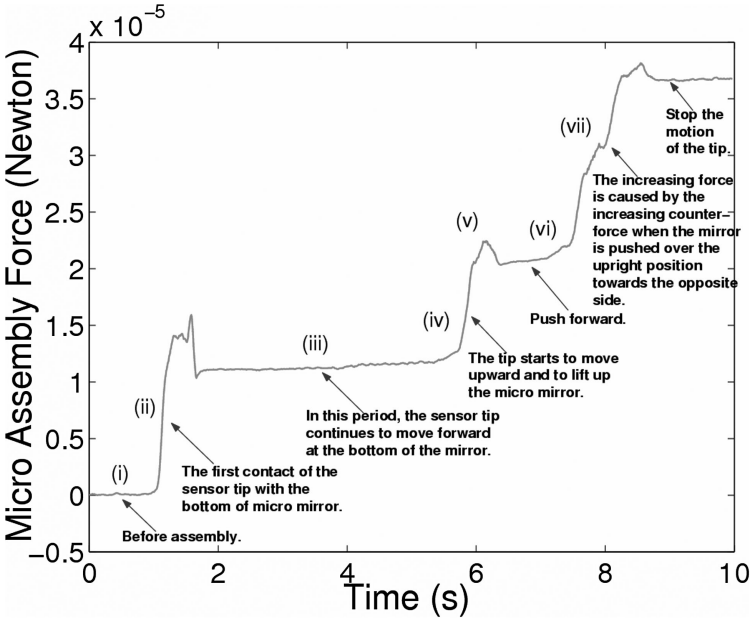

Figure 21. The feedback 1D micro-force during cooperative assembly of a micro-mirror *via* the Internet.

Based on the event-synchronization action, as shown in Fig. 21, the feedback 1D micro lift-up force in the assembly operations was approximately corresponding from (i) to (vii) in the feedback video sequence shown in Fig. 20.

Furthermore, the sequence in Fig. 22 demonstrates another human/robot cooperative microassembly between Hong Kong (remote operator side, using Phantom joystick) and USA (micro robot and work-cell side at MSU). In this operation, the PVDF 2D micro-force sensor was used with a gain K_c of 48. The sensor can detect and feed back the push-forward force (horizontal) and the lift-up force (vertical) during tele-assembly. The size of the assembled mirror is about 600 μm $\times$ 400 μm. In this operation, the microscope was set with a 10$\times$ objective lens, the force scale factor was 2.5×10^5.

Figure 23 shows the feedback 2D micro-forces in the assembly process. Using the event-synchronization, the force actions correspond to the video sequence in Fig. 22 very well. Figure 22a shows moving the sensor tip to the bottom of micro-mirror, Fig. 22b moving the tip forward to first contact the mirror bottom at about 1.2s, Fig. 22c at about 1.8 s, pushing and lifting the mirror up, and Fig. 22d lifting up and pushing forward the micro-mirror to upright position at about 2.5 s and then gradually and slowly lifting up the sensor tip away from the upright mirror from 2.5 to 5.0 s.

In Fig. 23, at about 2.0 s, a large spike in the lift-up force plot indicates that the lift-up force quickly increases when the tip was overcoming the large force from the moments of the hinges and the latch locks of mirror. The lift-up force then

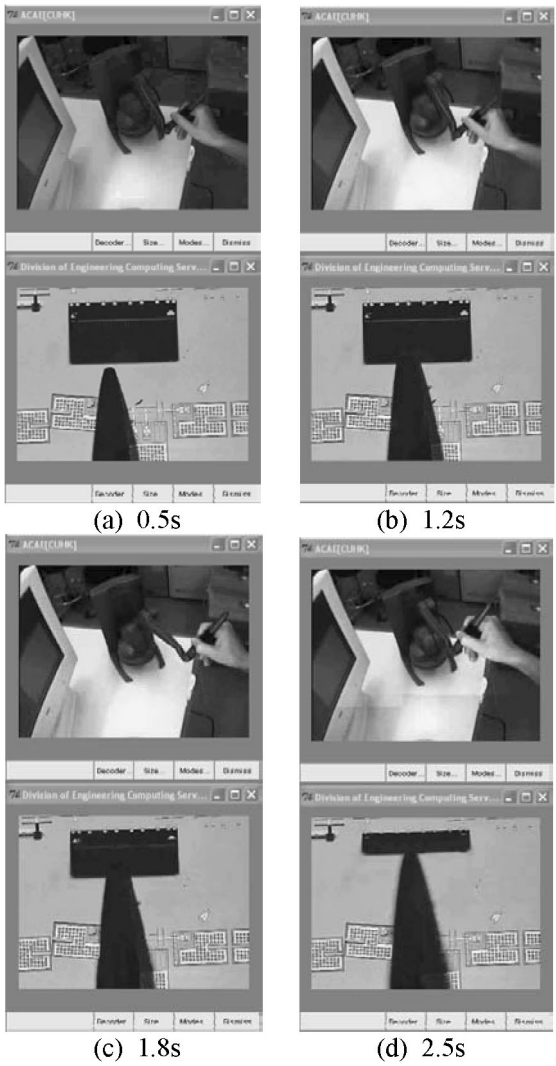

Figure 22. The feedback video sequence of human/robot cooperative tele-assembly of micro-mirror using a Phantom joystick and the 2D sensor set-up between USA (bottom: micro work-cell at MSU) and Hong Kong (top: remote operation side at CUHK).

decreases quickly when the mirror was approaching the upright position, while the push-forward force was increasing gradually due to the increasing counter force and moments from the hinges and latches. From about 2.5 to 5 s, the sensor tip was only lifting up gradually and slowly, and was leaving the upright mirror. The push-forward force was kept approximately to a constant, and the lift-up force continued to decrease to zero as the downward pressure from the mirror to the sensor tip gradually diminished.

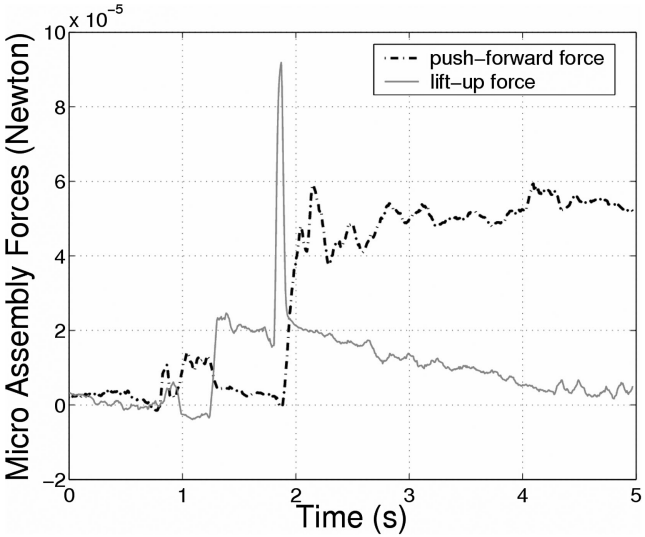

Figure 23. The feedback 2D micro forces during cooperative assembly of a micro-mirror *via* Internet.

By feeding back the scaled micro-force and the event-synchronized video *via* the Internet, the operator at the Hong Kong side had the synchronized haptic/force and visual feeling during the interactive operation. This feeling has greatly enhanced the success rate of the teleassembly of micro-mirrors and improved the reliability and dependability of human/robot cooperative microassembly. As demonstrated in the experiments, the developed networked human/robot cooperation can significantly increase the robustness, efficiency and safety of robotic operations in microassembly.

5. CONCLUSIONS

This paper presents the development of a networked human/robot cooperative environment for reliable and dependable microassembly. In this paper, based on integrating an *in situ* PVDF piezoelectric micro-force sensing tool with a resolution in the range of μN, and using the event-synchronization for the feedback of assembly video and micro-force, the developed networked human/robot cooperative platform can greatly advance applications in tele-microassembly. Internet based experimental results demonstrated the performance of the developed networked human/robot cooperative platform. Its applications could be an important step to enable reliable and high-yield batch fabrication and assembly of MEMS *via* local area network or Internet.

Acknowledgements

This research work was partially supported by USA NSF Grants IIS-9796300, IIS-9796287, EIA-9911077, OISE-0314120 and DMI-0500372, and also partially

supported by a grant from the Hong Kong Research Grants Council (CUHK 4381/02).

REFERENCES

1. K. F. Behringer, R. S. Fearing and K. Y. Goldberg, Microassembly, in: *The Handbook of Industrial Robotics*, 2nd edn, S. Nof (Ed.), pp. 1045–1066. Wiley, New York, NY (1999).
2. S. Fatikow, J. Seyfried, S. Fahlbusch, A. Buerkle and F. Schmoeckel, A flexible microrobot-based microassembly station, *Journal of Intelligent and Robotic Systems* **27**, 135–169 (2000).
3. Y. Murakami, K. Shibata, X. Zheng and K. Ito, Human Control characteristics in bilateral micro-teleoperation system, in: *The 26th Annual Conference of the IEEE on Industrial Electronics*, Nagoya, Volume 1, pp. 602–607 (2000).
4. B. Nelson, Y. Zhou and B. Vikramaditya, Sensor-based micro-assembly of hybrid MEMS devices, *IEEE Control Systems Magazine* **18**, 35–45 (1998).
5. W. Zesch, R. Fearing, Alignment of microparts using force controlled pushing, in: *1998 SPIE Conference on Microrobotics and Micromanipulation*, Boston, MA, pp. 148–156 (1998).
6. R. S. Fearing, Survey of sticking effects for micro parts handling, in: *Proceedings of 1995 IEEE/RSJ International Conference on Intelligent Robots and Systems*, Pittsburgh, PA, pp. 212–217 (1995).
7. M. Boukhnifer, A. Ferreira and J.-G. Fontaine, Scaled teleoperation controller design for micromanipulation over Internet, in: *Proceedings of the IEEE International Conference on Robotics and Automation*, New Orleans, LA, pp. 4577–4583 (2004).
8. N. Ando, P. T. Szemes, P. Korondi and H. Hashimoto, Improvement of response isotropy of haptic interface for tele-micromanipulation systems, in *Proceedings of the IEEE International Conference on Robotics and Automation*, Washington, DC, pp. 1925–1930 (2002).
9. A. Ferreira, Strategies of human–robot interaction for automatic microassembly, in: *Proceedings of the IEEE International Conference on Robotics and Automation*, Taipei, pp. 3076–3081 (2003).
10. A. Sano, H. Fujimoto and T. Takai, Human-Centered Scaling in Micro-Teleoperation, in: *Proceedings of the IEEE International Conference on Robotics and Automation*, Seoul, pp. 380–385 (2001).
11. K. Park, W. K. Chung and Y. Youm, Obtaining passivity of micro-teleoperation handling a small inertia object, in: *Proceedings of the IEEE International Conference on Robotics and Automation*, Washington, DC, pp. 3266–3271 (2002).
12. A. Codourey, M. Rodriguez and I. Pappas, A task-oriented teleoperation system for assembly in the microworld, in: *Proceedings of the International Conference on Advanced Robotics*, Monterey, CA, pp. 117–123 (1997).
13. B. Vikramaditya and B. J. Nelson, Modeling microassembly tasks with interactive forces, in: *Proceedings of the 4th IEEE International Symposium on Assembly and Task Planning*, Fukuoka, pp. 482–487 (2001).
14. Y. Yamamoto, R. Konishi, Y. Negishi and M. Arakawa, Tool development for force-feedback micro manipulation system, in: *Proceedings of the IEEE/RSJ International Conference on Intelligent Robots and Systems*, Las Vegas, NV, pp. 2254–2259 (2003).
15. S. K. Koelemijer, C. L. Benmayor, J.-M. Uehlinger and J. Jacot, Cost effective micro-system assembly automation, in: *Proceedings of Emerging Technologies and Factory Automation*, Barcelona, Vol. 1, pp. 359–366 (1999).
16. J. R. Reid, V. M. Bright and J. H. Comtois, Automated assembly of flip-up micromirrors, in: *TRANSDUCERS '97*, Chicago, IL, Vol. 1, pp. 347–350 (1997).
17. E. E. Hui, R. T. Howe and M. S. Rodgers, Single-step assembly of complex 3D microstructures, in: *IEEE MEMS 2000*, Miyazaki, pp. 602–607 (2000).

18. M. Carrozza, A. Eisinberg, A. Menciassi, D. Campolo, S. Micera and P. Dario, Towards a force-controlled microgripper for assembling biomedical microdevices, *Journal of Micromechanics and Microengineering* **10**, 271–276 (2000).
19. D. Kleinke and H. Uras, A magnetostrictive force sensor, *Review of Science Instruments* **65** (5), 1699–1710 (1994).
20. R. Anderson and M. Spong, Bilateral control of teleoperators with time delay, *IEEE Transactions on Automatic Control* **34**, 494–501 (1989).
21. W. Kim, B. Hannaford and A. Bejczy, Force-reflection and shared compliant control in operating telemanipulators with time delay, *IEEE Transactions on Robotics and Automation* **8**, 176–185 (1992).
22. N. Xi, *Event-based planning and control for robotic systems*, Doctoral Dissertation, Washington University at St. Louis, St. Louis, MO (1993).
23. I. Elhajj, N. Xi and Y.-H. Liu, Real-time control of internet based teleoperation with force reflection, in: *Proceedings of the 2000 IEEE International Conference on Robotics and Automation*, San Francisco, CA, pp. 3284–3289 (2000).
24. I. Elhajj, N. Xi, W. K. Fung, Y.-H. Liu, W. Li, T. Kaga and T. Fukuda, Haptic information in internet-based teleoperation, *IEEE Transactions on Mechatronics* **6** (3), 295–304 (2001).
25. *Piezo Film Sensors, Technical Manual, Internet Version*. Measurement Specialties, Hampton, VA (1998).
26. D. H. Kim, B. Kim, H. Kang and B. K. Ju, Development of a piezoelectric polymer-based sensorized microgripper for microassembly and micromanipulation, in: *Proceedings of 2003 IEEE International Conference on Robotics and Automation*, Taipei, pp. 1864–1869 (2003).
27. IEEE, *IEEE Standard on Piezoelectricity, ANS/IEEE Standard 176–1987*. IEEE, New York, NY (1987).
28. W. H. Bowes, L. T. Russell and G. T. Suter, *Mechanics of Engineering Materials.* Wiley, New York, NY (1984).
29. Y. T. Shen, N. Xi and W. J. Li, Modeling and control of a flexible sensor structure in microassembly, in: *The 16th IFAC World Congress*, Tu-E19-TO/3, Prague, Czech Republic, Sendai (2005).
30. Y. T. Shen, N. Xi, U. Wejinya and W. J. Li, High sensitivity 2-D force sensor for assembly of surface MEMS devices, in: *Proceedings of 2004 IEEE/RSJ International Conference on Intelligent Robots and Systems*, Sendai, Volume 4, pp. 3363–3368 (2004).
31. S. McCanne and V. Jacobson, VIC: a flexible framework for packet video, in: *Proceedings of the ACM International Multimedia Conference Exhibition*, San Francisco, CA, pp. 511–522 (1995).
32. N. Hogan, Multivariable mechanics of the neuromuscular system, in: *IEEE 8th Annual Conference of Engineering in Medicine and Biology Society*, New York, NY, pp. 594–598 (1986).
33. T. Milner, Human operator adaptation to machine instability, in: *Advances in Robotics, Mechatronics and Haptic Interfaces*, pp. 698–709. ASME, New York, NY (1993).
34. Y. T. Shen, N. Xi and W. J. Li, Force guided assembly of micro-mirrors, in: *Proceedings of the IEEE/RSJ International Conference on Intelligent Robots and Systems*, Las Vegas, NV, Volume 3, pp. 2149–2154 (2003).
35. T. J. Tarn, Y. Y. Wu, N. Xi and A. Isidori, Force regulation and contact transition control, *IEEE Control Systems Magazine* **6**, 32–40 (1996).
36. R. Kress, W. R. Hamel, P. Murray and K. Bills, Control strategies for teleoperated Internet assembly, *IEEE/ASME Transactions on Mechatronics* **6** (4), 410–416 (2001).
37. Y. Zhou, B. J. Nelson and B. Vikramaditya, Fusing force and vision feedback for micromanipulation, in: *Proceedings of the IEEE International Conference on Robotics and Automation*, Leuven, pp. 1220–1225 (1998).

38. I. Elhajj, N. Xi, B. H. Song, M.-M. Yu, W. T. Lo and Y. H. Liu, Transparency and synchronization in supermedia enhanced Internet-based teleoperation, in: *Proceedings of the IEEE International Conference on Robotics and Automation*, Washington, DC, pp. 2713–2718 (2002).

ABOUT THE AUTHORS

Yantao Shen received both the B.Eng. degree in Mechanical and Electrical Engineering and the M.Eng. degree in Mechatronic Control and Automation from Beijing Institute of Technology (Beijing, China). He received his Ph.D. degree specializing in robotics from The Chinese University of Hong Kong in 2002. Since 2002, he has been a research associate in the Department of Electrical and Computer Engineering at Michigan State University. Dr. Shen has published more than 40 papers in professional journals and conference proceedings in the fields of robotics and automation. Dr. Shen is also a finalist of Best Vision Paper Award at the IEEE International Conference on Robotics and Automation in 2001. Currently, his research interests include sensorized micro systems, smart sensors and actuators, visual servo systems and haptic/tactile interfaces.

Ning Xi received his D.Sc. degree in Systems Science and Mathematics from Washington University (St. Louis, MO, USA) in December 1993. He received his M.S. degree in Computer Science from Northeastern University (Boston, MA, USA) and his B.S. degree in Electrical Engineering from Beijing University of Aeronautics and Astronautics. Currently, he is John D. Ryder Professor of Electrical and Computer Engineering in the Department of Electrical and Computer Engineering at Michigan State University. Dr. Xi received the Best Paper Award at the IEEE/RSJ International Conference on Intelligent Robots and Systems in August, 1995. He also received the Best Paper Award in the 1998 Japan–USA Symposium on Flexible Automation. Dr. Xi was awarded the first Early Academic Career Award by the IEEE Robotics and Automation Society in May 1999. In addition, he is also a recipient of National Science Foundation CAREER Award. Currently, his research interests include robotics, manufacturing automation, micro/nano systems, and intelligent control and systems.

Booheon Song received both his B.S. degree in Computer Science and Engineering and his M.S degree in Electrical Engineering from Michigan State University (East Lansing, MI, USA). He is currently a team leader at Accenture. His research interests include Internet-based robotics and event-based systems.

Wen J. Li is with the Department of Automation and Computer-Aided Engineering, and currently heads the Centre for Micro and Nano Systems at The Chinese University of Hong Kong (CUHK). He received B.S. and M.S. degrees in Aerospace Engineering from the University of Southern California and his Ph.D. degree specializing in MEMS from the University of California Los Angeles. Before joining CUHK, he held R&D positions at the NASA Jet Propulsion Laboratory (Pasadena, CA, USA) and The Aerospace Corporation (El Segundo, CA, USA). His research group has won best paper awards at premier conferences of

the IEEE Nanotechnology Council (IEEE-NANO) and the IEEE Robotics and Automation Society (IEEE-ICRA) in 2003 for its work on micro cell-grippers and nano-sensors. The group's work on nanotube sensors has recently gained significant international interest and, hence, he has presented several keynote and invited talks in the USA, Taiwan, Canada and Europe in 2005. He has served as a guest editor for *IEEE Transactions on Automation Science and Engineering* and *IEEE/ASME Transactions on Mechatronics*. He has been appointed to serve as the General Chair of IEEE Nano 2007 by the IEEE Nanotechnology Council. He is also a Distinguished Overseas Scholar of the Chinese Academy of Sciences.

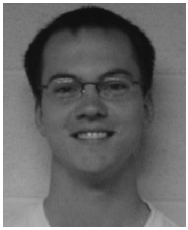

Craig A. Pomeroy is currently working towards a B.S. degree in Electrical Engineering at Michigan State University (East Lansing, MI, USA). He is currently a Research Assistant with the Robotics and Automation Laboratory, Department of Electrical Engineering, Michigan State University. His research interests include embedded systems, robotics, real-time systems and controls.